(Preprint) AAS 25-353

DETECTING UNSTABLE RESONANT ORBITS VIA KEPLERIAN MAP

Shohei Morimitsu[*], **Mai Bando**[†], and **Shinji Hokamoto**[‡]

Periodic orbits for the circular restricted three-body problem (CRTBP) are important in orbit design because they allow spacecraft to travel without fuel consumption. Currently, Newton's method is used to obtain the periodic orbit, but it is numerically very unstable and requires a large computational cost. In this study, we analyze the instability of periodic orbit calculation for the CRTBP on the Poincaré map and on the periapsis map, and show that the instability is reduced by performing periodic orbit calculation on the periapsis map.

INTRODUCTION

The circular -restricted three-body problem (CRTBP) is a model of the motion of a mass point under the gravity of two celestial bodies moving in a circular orbit around their barycenter, and is used to design spacecraft trajectories under the Earth-Moon gravity. The CRTBP has five equilibrium points,[1] and periodic orbits exist around the equilibrium points. These periodic orbits are of great interest in trajectory design because spacecraft can travel without consuming fuel, since they allows spacecraft to move periodically by natural forces alone. In addition, the stable and unstable manifolds associated with these periodic orbits provide pathways for designing low-energy trajectories, enabling efficient exploration in multi-body systems.

There are several numerical methods to calculate such periodic orbits. The standard method is the differential correction,[2] a type of the Newton-Raphson method. While this method can compute periodic orbits with high accuracy, it often suffers from computational instability and the need for a highly accurate initial guess. An analytical method called the Lindstedt-Poincaré method[3] provides a high-precision initial guess, and a numerical continuation[4] can be used to extend the solution. However, these methods also have limitations: The Lindstedt-Poincaré method is primarily applicable to periodic orbits near equilibrium points and may not be suitable for more complex orbits far from these points. Numerical continuation, while powerful for extending known solutions, can suffer from convergence issues when tracking orbits through bifurcations or other dynamical transitions.

A phenomenon known as the Newton fractal is observed when using the Newton method to find solutions.[5,6] This occurs when the Newton method is applied to problems in two or more dimensions, resulting in a complex boundary pattern. As shown in Figure 1, color-coding the regions according to their converged solutions reveals intricate structures, including boundaries and regions

[*]Master Student, Department of Aeronautics and Astronautics, Kyushu University, 819-0395 Fukuoka Japan, mormitsu.shohei.655@s.kyushu-u.ac.jp.

[†]Professor, Department of Aeronautics and Astronautics, Kyushu University, mbando@aero.kyushu-u.ac.jp.

[‡]Professor, Department of Aeronautics and Astronautics, Kyushu University, hokamoto@aero.kyushu-u.ac.jp.

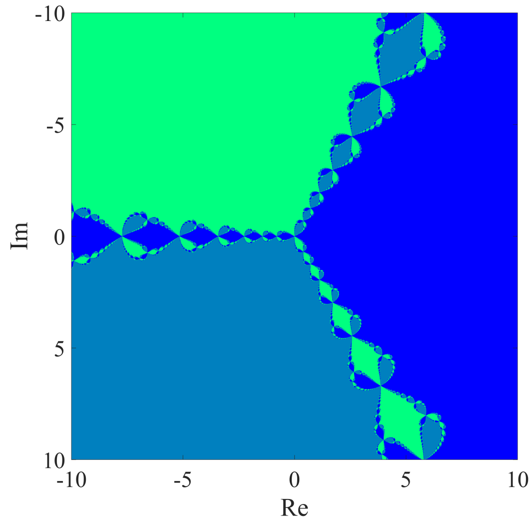

Figure 1: Newton fractal of $z^3 = 1$

resembling enclaves. As illustrated in Figure 1, the Newton method does not always converge to the nearest solution. Instead, it can exhibit convergence to distant solutions, resulting in these complex patterns. This phenomenon can be interpreted as a manifestation of the complexity and instability inherent in the original dynamical system when solved using the Newton method. The Newton fractal provides insights into the properties of the Newton method within a dynamical system, such as its convergence behavior and the radius of convergence.

The objective of this study is to explore the Newton fractal that arises during the detection of unstable periodic orbits in the CRTBP using the Newton method and clarify the differences in the complexity of basin structures depending on the method used for UPO computation. In this study, the periapsis map, an area-conserving map, is used as the Poincaré map to reduce the dimension of the system, while the Poincaré section at $y = 0$, which is often used, is not an area-conserving map. Diakonos method is one of the same root-finding algorithms similar to the Newton method. However, unlike the Newton method, which requires the calculation of first-order derivatives (i.e., the Jacobian matrix) for each iteration, the Diakonos method utilizes the system's underlying dynamics to guide the convergence process. This eliminates the need for derivative evaluations, which can be computationally expensive, particularly for complex systems like the CRTBP. As a result, the Diakonos method is expected to reduce computational costs and alleviate the numerical instability often associated with root-finding algorithms like Newton method. In this paper, we compare the corrections for periodic orbit calculations on the Poincaré map and on the periapsis map between the Newton method and the Diakonos method. As a further development, we also show that periodic orbits can be easily obtained using the Keplerian map, which is an approximation of the periapsis map.[7]

THEORIES

PCRTBP

In the CRTBP, we consider two planets P_1, P_2 and mass point P_3. The main bodies P_1 and P_2 move in a circular motion around the barycenter. The mass P_3 does not affect the movement of the two planets. When the motion is restricted to the in-plane motion, planar circular restricted three-body problem (PCRTBP) is expressed as

$$\begin{aligned}\ddot{x} - 2\dot{y} - x &= \frac{(1-\mu)(x+\mu)}{r_1^3} - \frac{\mu(x-1+\mu)}{r_2^3} \\ \ddot{y} + 2\dot{x} - y &= \frac{(1-\mu)y}{r_1^3} - \frac{\mu y}{r_2^3}\end{aligned} \tag{1}$$

where r_1, r_2 and μ are defined as

$$r_1 = \sqrt{(x+\mu)^2 + y^2} \tag{2}$$

$$r_2 = \sqrt{\{x - (1-\mu)\}^2 + y^2} \tag{3}$$

$$\mu = \frac{M_2}{M_1 + M_2} \tag{4}$$

The Jacobi constant C is defined as

$$U = \frac{1}{2}(x^2 + y^2) + \frac{1-\mu}{r_1} + \frac{\mu}{r_2} + \frac{1}{2}\mu(1-\mu) \tag{5}$$

$$C = 2U - (\dot{x}^2 + \dot{y}^2) \tag{6}$$

Periodic orbit calculations for PCRTBP

The periodic orbit calculation for PCRTBP follows this flow (see Fig.2).

1. Determine the initial estimated solution.
2. Using Eq.(1), it propagates the trajectory and stops when the stopping condition is met.
3. The initial values are modified using a quadrature algorithm so that the difference between the initial and final states is zero.
4. The above procedure is repeated until the orbit closes.

This study employs the following two stopping conditions.

1. When $y = 0$ and $\dot{y} < 0$ for the Nth time (Poincaré section with $y = 0$)
2. When $\dot{r}_1 = 0$ and $\ddot{r}_1 > 0$ (Earth perigee) for the Nth time (periapsis map)

The root-finding algorithm also deals with the Newton and Diakonos method.[8]

Diakonos Method

Diakonos method is a method for calculating unstable periodic orbits in chaotic dynamical systems. In this method, given a N-dimensional discrete chaotic dynamical system $U : \boldsymbol{r}_{i+1} = \boldsymbol{f}(\boldsymbol{r}_i)$, the periodic orbit is computed by stabilizing its unstable fixed points by a transformation L_k. Specifically, consider the following dynamical system

$$\boldsymbol{r}_{i+1} = \boldsymbol{r}_i + \boldsymbol{\Lambda}_k(\boldsymbol{f}(\boldsymbol{r}_i) - \boldsymbol{r}_i) \tag{7}$$

where $\boldsymbol{\Lambda}_k = \lambda \boldsymbol{C}_k$ satisfies the following properties

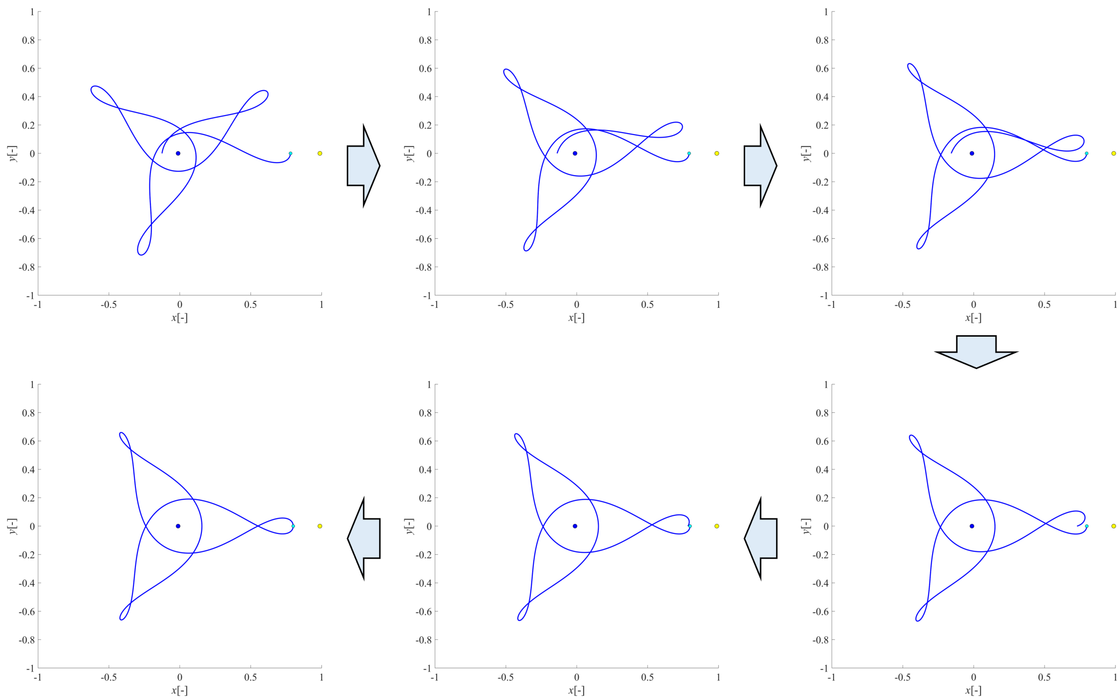

Figure 2: Periodic orbit calculation

1. λ is a constant and satisfies $0 < \lambda \ll 1$.
2. $\boldsymbol{C}_k$ is an $N \times N$ matrix.
3. The elements of $\boldsymbol{C}_k$ are $C_{ij} \in \{0, \pm 1\}$, with only one non-zero element in each row and column.

$\boldsymbol{C}_k$ that stabilizes an unstable fixed point depends on the type of fixed point and is discovered by experimentation.

Poincaré Map

The Poincaré map is a method used to analyze chaotic systems. In this approach, a set of random initial points is chosen, and their values are iteratively mapped and plotted. The Poincaré map reveals regions with circumferential patterns that repeat (torus regions) and areas where points are scattered irregularly, forming unclear shapes (chaotic regions).

Periodic orbits are found in both the torus and chaotic regions. Periodic orbits in the torus region are stable, while those in the chaotic region are unstable. Generally, unstable periodic orbits are challenging to compute, and the periodic orbits considered in this study are also unstable.

Analysis method of convergence radius using modification quantities

To evaluate the radius of convergence for periodic orbit calculations, this paper utilizes a color map representing the magnitude of the corrections computed by the root-finding algorithm. The map is generated by dividing a two-dimensional space into a grid and calculating the magnitude of the correction for each grid point.

In this color map, points where the correction magnitude is zero correspond to periodic orbits. The regions surrounding these points, where the magnitude of the correction increases gradually, indicate areas where convergence to the periodic orbit is expected.

Keplerian map

The approximation of the periapsis map for PCRTBP is given by the Keplariam map.[7]

$$\begin{cases} p_{n+1} = p_n + \mu f(p_n, \theta_n) \\ \theta_{n+1} = \theta_n - 2\pi(-2p_{n+1})^{-\frac{3}{2}} \pmod{2\pi} \end{cases} \tag{8}$$

where $f(p_n, \theta_n)$ is the kick function. Also, p_n has the following relationship with a_n.

$$p_n = -\frac{1}{2a_n} \tag{9}$$

Furthermore, it is assumed that the kick function $f(p_n, \theta_n)$ depends only on θ_n and considers the following mapping

$$\begin{cases} p_{n+1} = p_n + \mu f(\theta_n) \\ \theta_{n+1} = \theta_n - 2\pi(-2p_{n+1})^{-\frac{3}{2}} \pmod{2\pi} \end{cases} \tag{10}$$

This map is called a Keplerian map and represents an approximation of the periapsis map when a is fixed to a certain value.

RESULTS

The PCRTBP is reduced to a two-dimensional map by fixing the Jacobi constant and using the stopping condition.

First, we compare the modifications of each root-finding algorithm for the case of $y = 0$ and $\dot{y} < 0$ Poincaré sections and for the case of periapsis map. Figures 4 and 5 respectively show the Poincaré map for the case where $y = 0$ and $\dot{y} < 0$ and where the proximal point is used as the stopping condition. The points on the map of periodic orbits in Fig.3 are marked with red markers to compare the properties when the same periodic orbit is obtained. Other periodic orbits obtained for the same order number are shown with white markers.

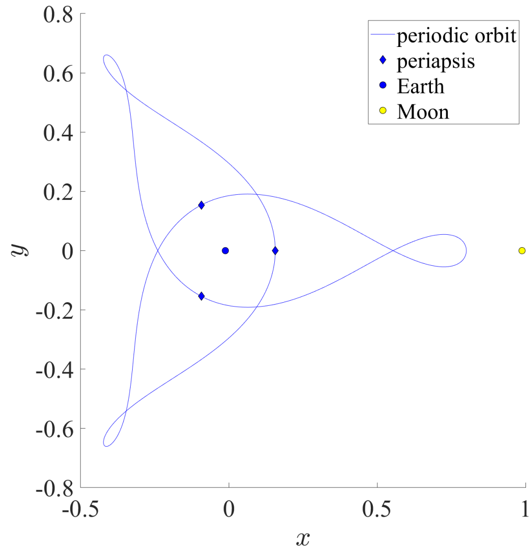

Figure 3: Periodic Orbits to Compare Convergence Radii

Table 1: Simulation Condition for the Poincare Map with $y = 0$ and $\dot{y} < 0$

Stop Condtion	$y = 0$ and $\dot{y} < 0$
Relative Mass μ	0.0121536
Jacobi Constant	3.1678
Domain of Definition	$x \in [-0.4, 1.2]$ $\dot{x} \in [-2, 2]$
Grid Number	1001×1001
Number of Times$N$	3

Table 2: Simulation Condition for the Periapsis Map

Stop Condition	$\dot{r}_1 = 0$ and $\dot{r}_1 > 0$
Relative Mass μ	0.0121536
Jacobi Constant	3.1678
Domain of Definition	$\theta \in [-\pi, \pi]$ $a \in [0.35, 0.65]$
Grid Number	1001×1001
Number of Times$N$	3

Tables 1 and 2 summarize the simulation conditions for the Poincaré map ($y = 0$, $\dot{y} < 0$) and the Periapsis map. The magnitudes of the modifications calculated by Diakonos and Newton methods for these two simulation conditions are shown in Figs.6-9. Figs.6-9 illustrate that the magnitude of modification depends significantly on the root-finding algorithm and stopping condition, even for the same periodic orbit. Between the two methods, the periapsis map shows a slower increase in the magnitude of modification near the periodic orbit compared to the Poincaré section at $y = 0$ and $\dot{y} < 0$. Therefore, a wider range of initial values for easy convergence can be expected. The comparison of the root-finding algorithms is not possible to determine from these figures which root-finding algorithm is superior in terms of convergence radius, because the trend is reversed depending on the method of taking the Poincaré section.

Then, the Diakonos and Newton methods are actually iterated over and over again to examine the basins of attraction, which are color-coded according to the points of convergence. The coefficient

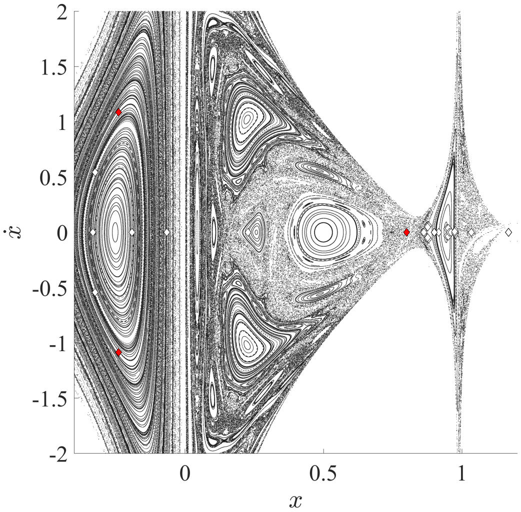

Figure 4: Poincaré Map when $y = 0$.

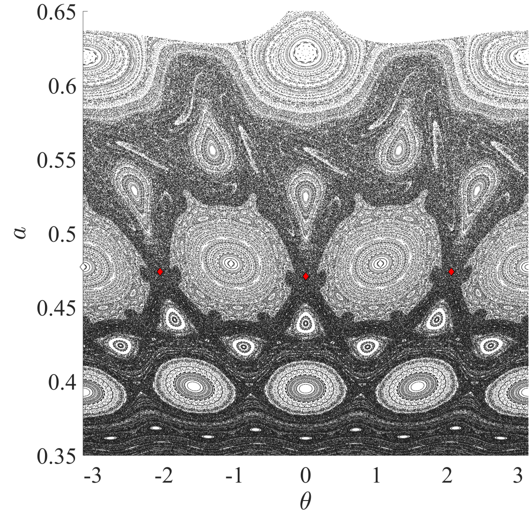

Figure 5: Periapsis Map

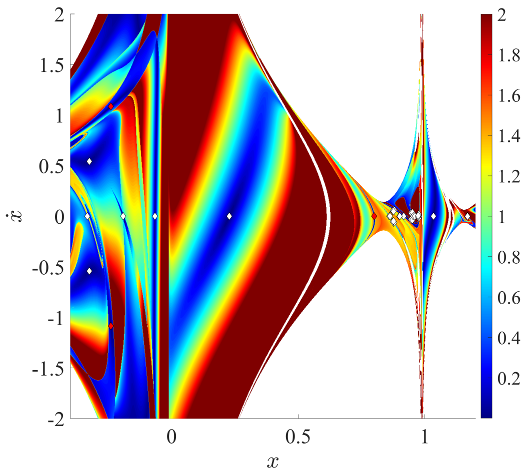

Figure 6: Amount of modification by Diakonos method in the Poincaré Map for $y = 0$

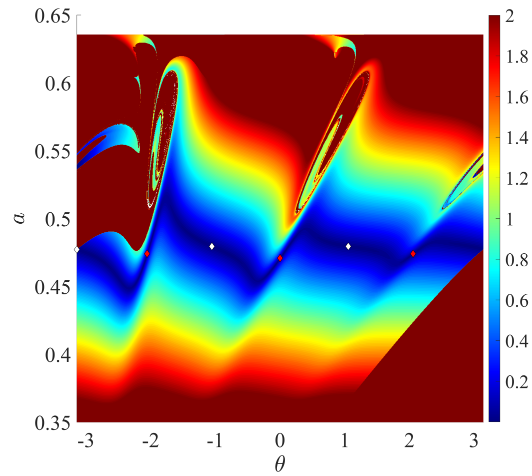

Figure 7: Amount of modification by Diakonos method in Periapsis Map

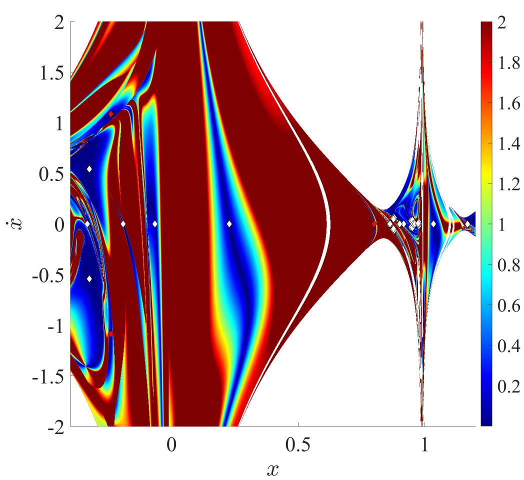

Figure 8: Amount of modification by Newton method in the Poincaré Map for $y = 0$

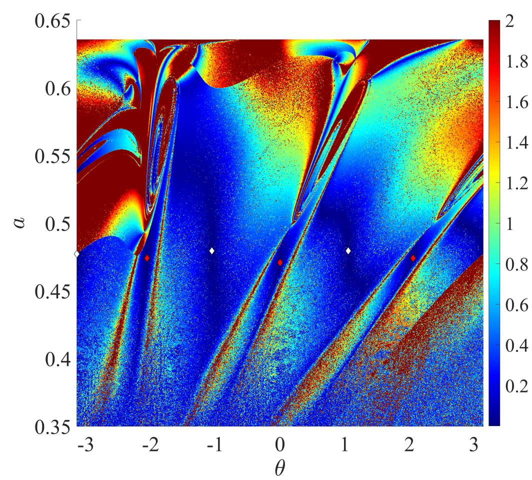

Figure 9: Amount of modification by Newton method in Periapsis Map

matrix $\mathbf{\Lambda}_k$ of the Diakonos method is

$$\begin{bmatrix} 0.1 & 0 \\ 0 & -0.1 \end{bmatrix} \text{ (i)}, \quad \begin{bmatrix} 0.1 & 0 \\ 0 & -0.1 \end{bmatrix} \text{ (ii)}, \quad \begin{bmatrix} -0.1 & 0 \\ 0 & 0.1 \end{bmatrix} \text{ (iii)}, \quad \begin{bmatrix} -0.1 & 0 \\ 0 & -0.1 \end{bmatrix} \text{ (iv)}$$

The number of iterations is evaluated in four cases: 1000 iterations for the Diakonos method (non-convergence after 100 iterations) and 100 or 1000 iterations for the Newton method. The results for the case of Poincaré sections with $y = 0$ and $\dot{y} < 0$ are shown in Fig.10. The results for the case of periapsis map are shown in Fig.11. Also, the calculated periodic orbits are shown in Fig.12. First, when the Newton method is used on the Poincaré section with $y = 0$, the periodic orbit of the target Fig.3 does not converge. This may be because the convergence radius is too small and there is no initial point of convergence. Comparing the methods, the Diakonos method tends to have a wider convergence radius. On the other hand, the Newton method also has a large enough convergence radius for the periapsis map. Comparing the two methods in terms of Poincaré cross sections, the periapsis map has a larger radius of convergence for the periodic orbit of the target. In the case of the Poincaré section taken at $y = 0$, the number of periodic orbits in the section is large, and the radius of convergence of the periodic orbit we want to find is narrowed. Comparing the fractal with the Newton method, the $y = 0$ Poincaré cross section hardly converges in 100 iterations, whereas the periapsis map does. This is because the $y = 0$ Poincaré cross section updates its solution very slowly along the dark blue region in Fig.8. Therefore, when comparing the convergence speed with the Diakonos method, the Newton method is the only one that converges in less than 100 iterations for the periapsis map, which is superior to the Diakonos method. Comparing the magnitude of the modification with that shown in the figure, the trend is similar in Fig.10a and Fig.11e, where there are many periodic orbitals to be obtained, but not in the other cases. However, in other cases, they are not similar. This indicates that predicting the convergence radius based on the magnitude of modification is effective for the Newton method, which consistently converges to periodic orbits, but less effective for the Diakonos method.

Next, we investigate the calculation of periodic orbits in the Keplerian map, represented by Eq.(10). First, the simulation conditions are summarized in Table 3, and the Keplerian map, approximated by the periodic orbit with orbit length radius $a = 0.4079$, is depicted in Fig.13. In this figure, the triangular markers indicate periodic orbits in the periapsis map, while the diamond markers represent periodic orbits in the Keplerian map. The deviation between these markers arises from approximation errors inherent in the Keplerian map. The magnitude of the modifications computed using the Diakonos and Newton methods is presented in Figs.7 and 15, respectively, while the basins of attraction are shown in Fig.16. When comparing these figures with those of the periapsis map, similar trends are observed, except for cases (ii) and (iii) of the Diakonos method. In these cases, the solutions converge to different fixed points. This discrepancy suggests that the nature of the fixed point around $\theta = 2.1$ may have changed. Unlike the periapsis map, the Keplerian map no longer exhibits the noisy enclaves seen previously. This difference may be attributed to the Keplerian map's ability to calculate more smoothly the parts of the orbit that were poorly computed in the periapsis map. In the periapsis map, the nonlinearities of the planar circular restricted three-body problem (PCRTBP) often caused the orbit to leave the Earth-Moon gravitational sphere or collide with the Earth or Moon.

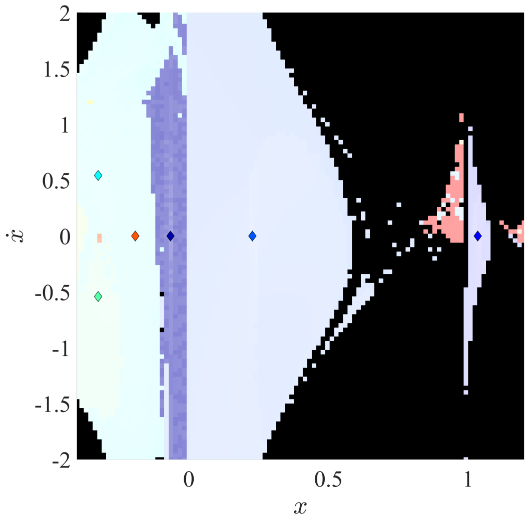

(a) Diakonos fractal in the Poincaré Map for $y = 0$ (i)

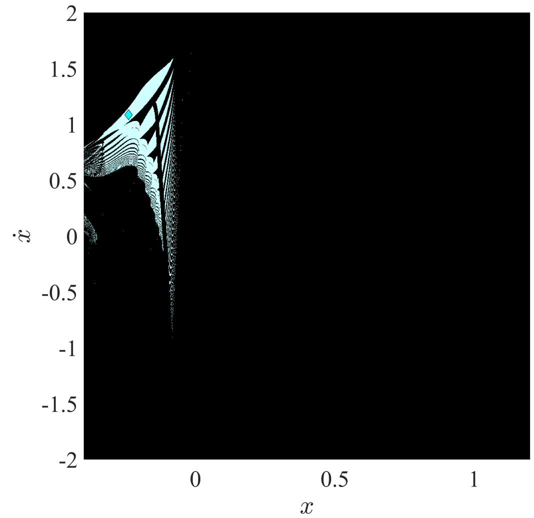

(b) Diakonos fractal in the Poincaré Map for $y = 0$ (ii)

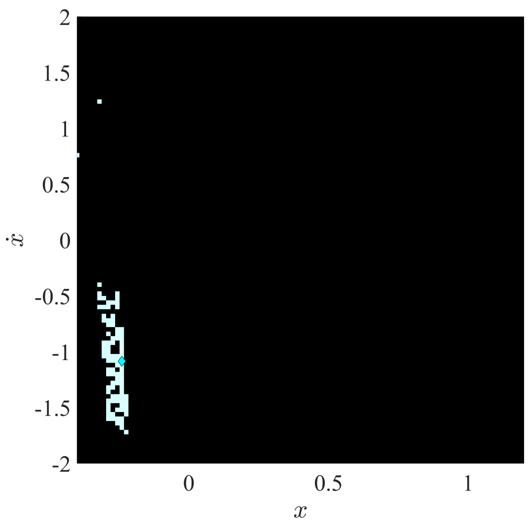

(c) Diakonos fractal in the Poincaré Map for $y = 0$ (iii)

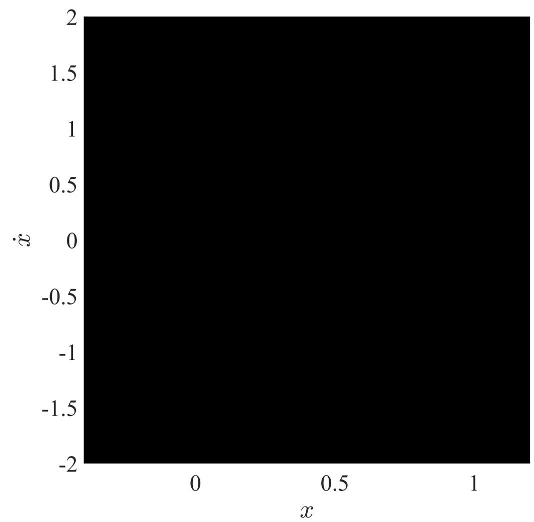

(d) Diakonos fractal in the Poincaré Map for $y = 0$ (iv)

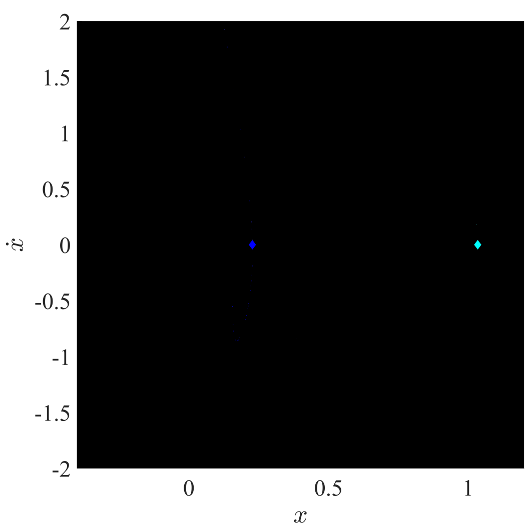

(e) Newton fractal for 100 iterations in the Poincaré Map with $y = 0$

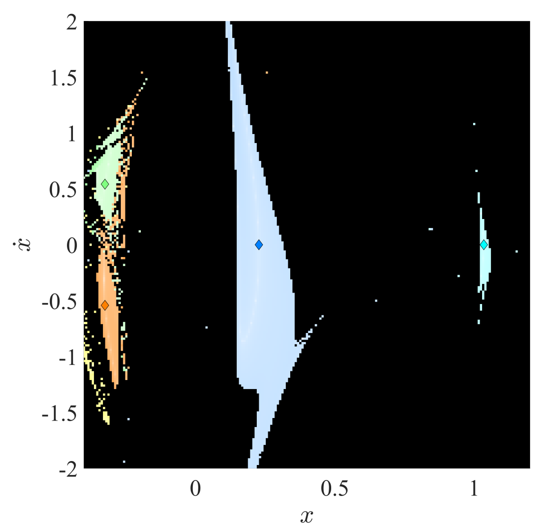

(f) Newton fractal for 1000 iterations in the Poincaré Map with $y = 0$

Figure 10: Fractals in the Poincaré Map for $y = 0$

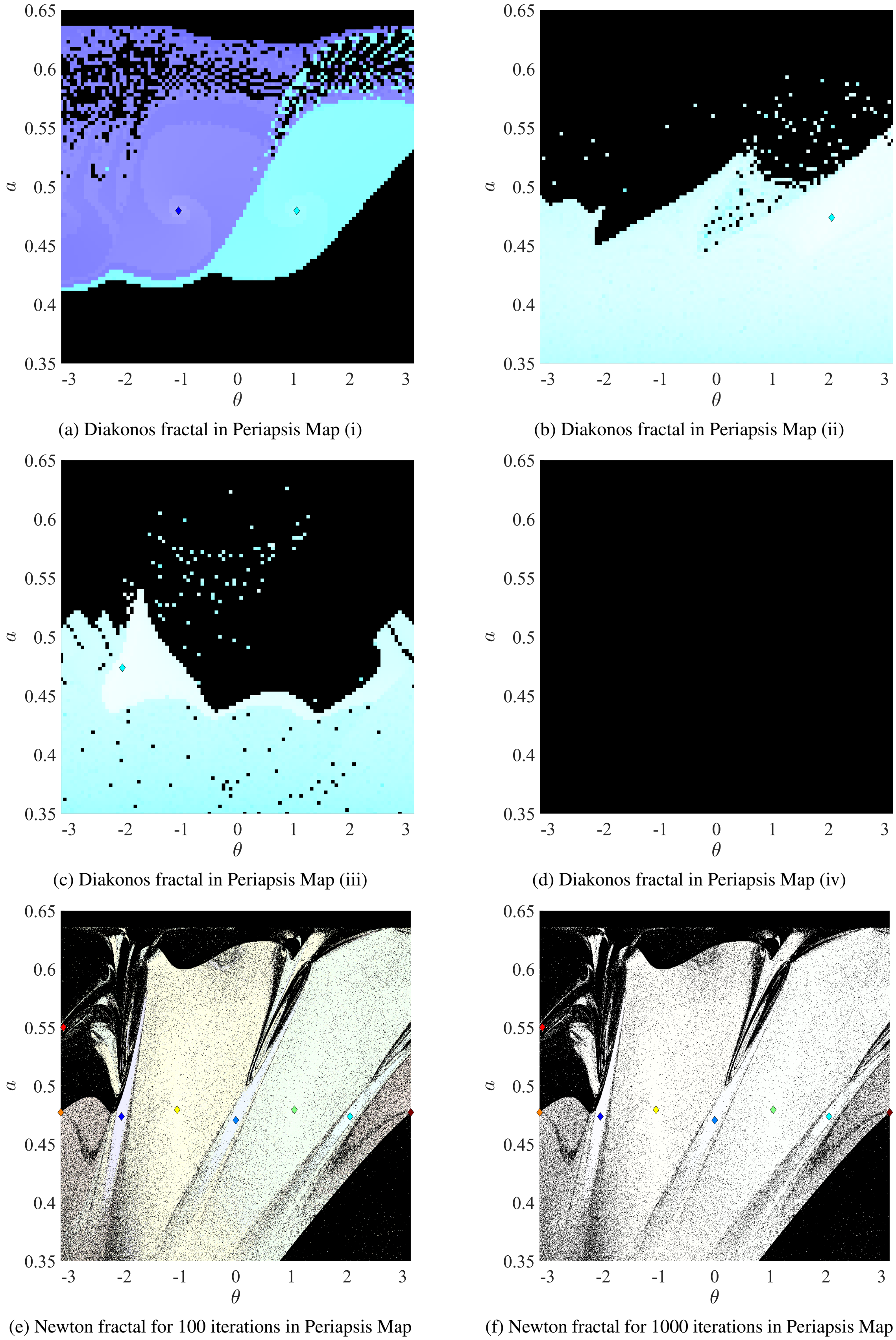

(a) Diakonos fractal in Periapsis Map (i)

(b) Diakonos fractal in Periapsis Map (ii)

(c) Diakonos fractal in Periapsis Map (iii)

(d) Diakonos fractal in Periapsis Map (iv)

(e) Newton fractal for 100 iterations in Periapsis Map

(f) Newton fractal for 1000 iterations in Periapsis Map

Figure 11: Fractals in Periapsis Map

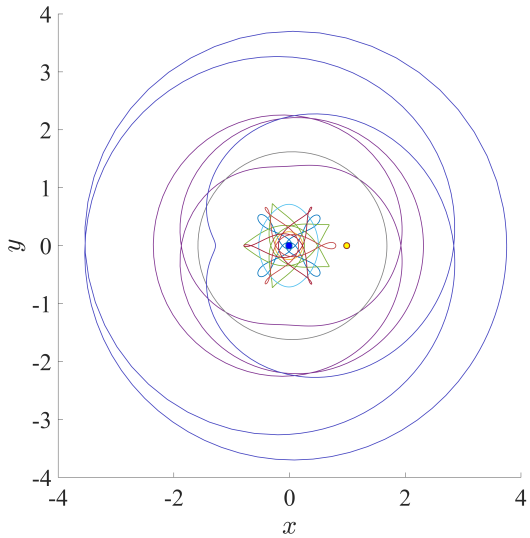

(a) Periodic Orbits calculated by Diakonos method in the Poincaré Map for $y = 0$

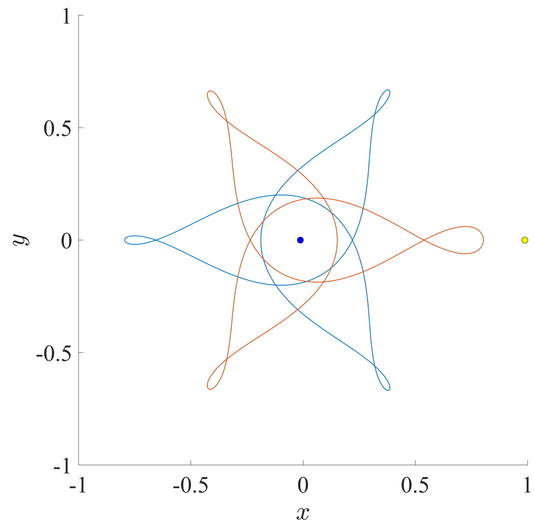

(b) Periodic Orbits calculated by Diakonos method in Periapsis Map

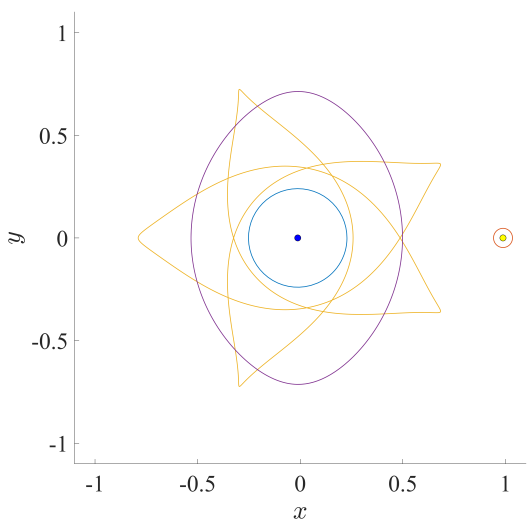

(c) Periodic Orbits calculated by Newton method in the Poincaré Map for $y = 0$

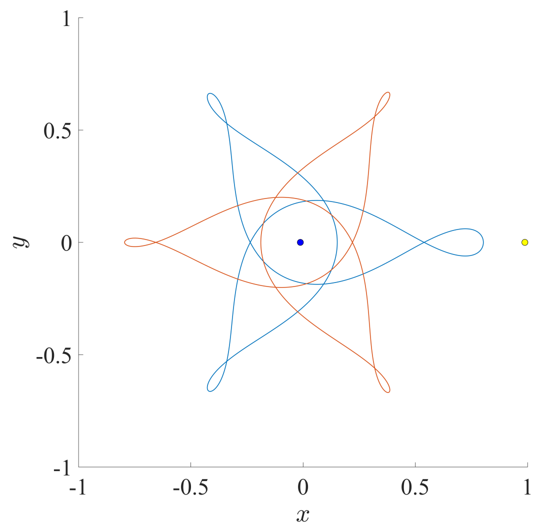

(d) Periodic Orbits calculated by Newton method in Periapsis Map

Figure 12: Calculated Periodic Orbits

Table 3: Simulation Condition for the Keplerian Map

Semi-Major Axis a	0.4079
Relative Mass μ	0.0121536
Jacobi Constant	3.1678
Domain of Definition	$\theta \in [-\pi, \pi]$ $a \in [0.35, 0.65]$
Grid Number	1001×1001
Number of Times$N$	3

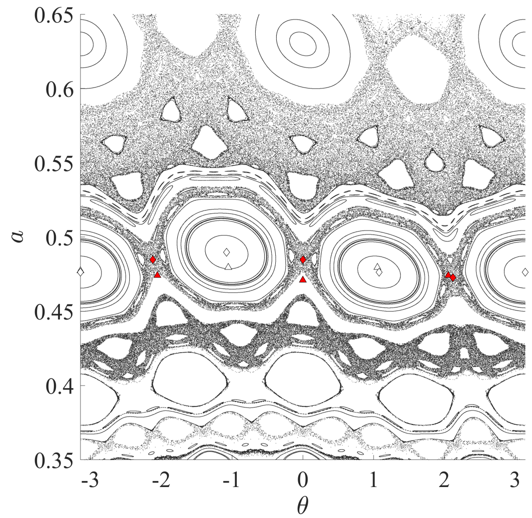

Figure 13: Keplerian Map approximated by $a = 0.4079$

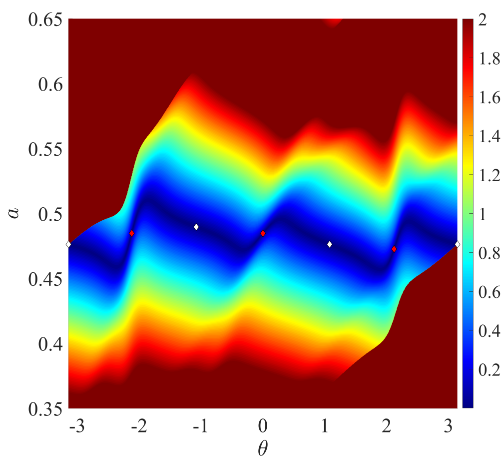

Figure 14: Amount of modification by Diakonos method in Keplerian Map

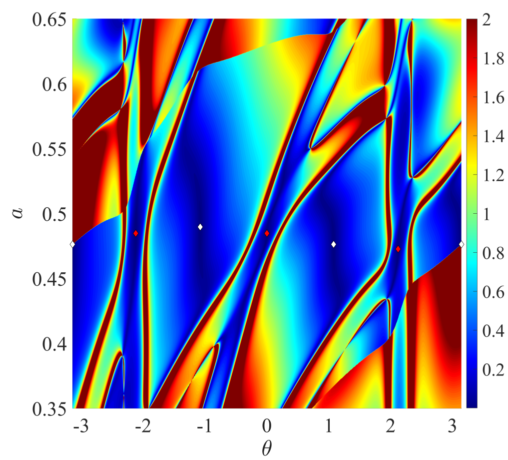

Figure 15: Amount of modification by Newton method in Keplerian Map

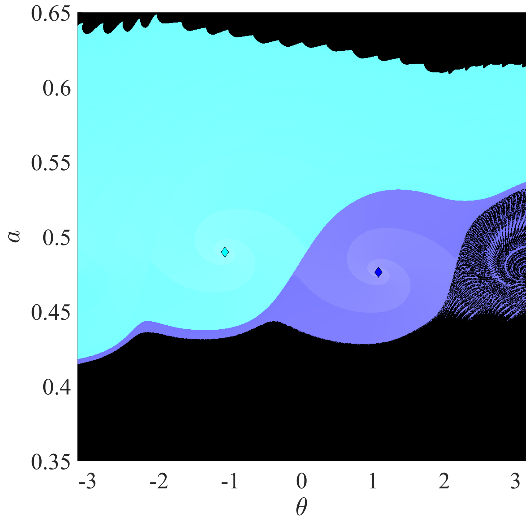

(a) Diakonos fractal in Keplerian Map (i)

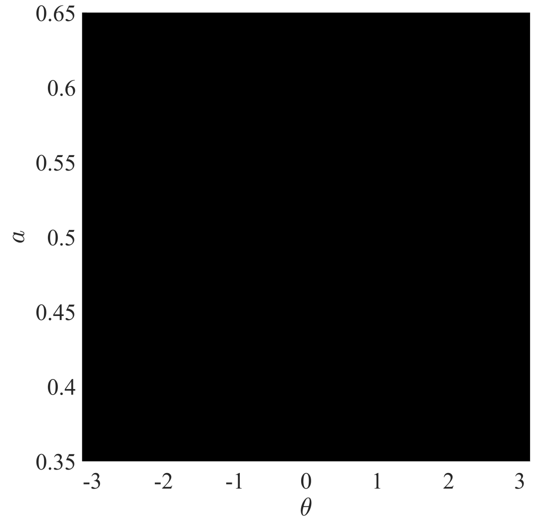

(b) Diakonos fractal in Keplerian Map (ii)

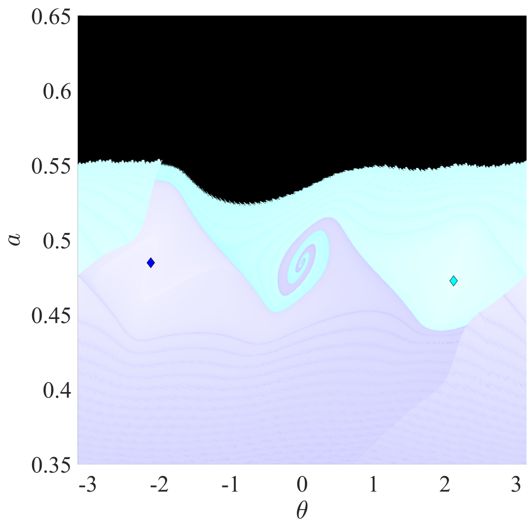

(c) Diakonos fractal in Keplerian Map (iii)

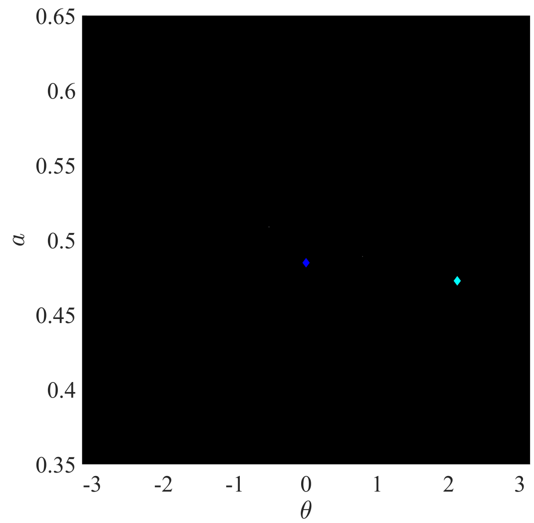

(d) Diakonos fractal in Keplerian Map (iv)

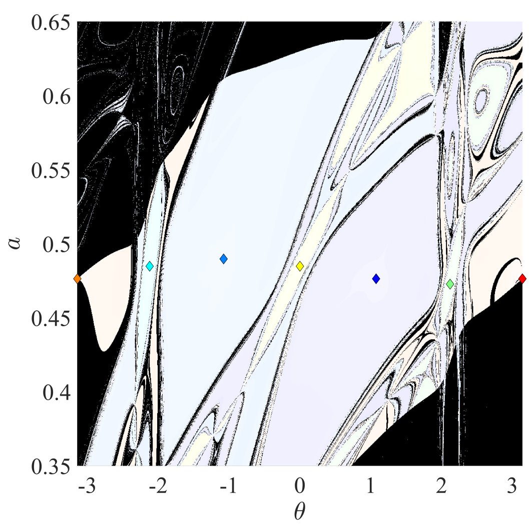

(e) Newton fractal for 100 in Keplerian Map

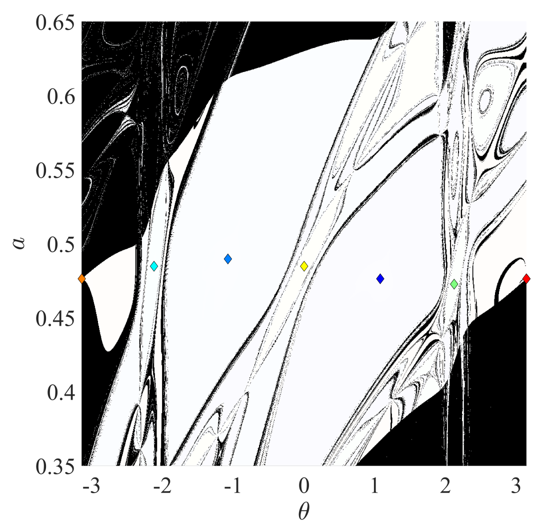

(f) Newton fractal for 1000 in Keplerian Map

Figure 16: Fractals for 1000 in Keplerian Map

CONCLUDING REMARKS

In this paper, we compare the magnitude of corrections between the Diakonos method and the Newton method on the Poincaré map and the periapsis map to evaluate the radius of convergence, a key factor in calculating periodic orbits for the circular restricted three-body problem.

The results indicate that the periapsis map combined with the Diakonos method demonstrates superior performance in terms of convergence radius. However, even with the Newton method, the periapsis map exhibits a sufficiently large convergence radius along with excellent convergence speed.

Furthermore, when the magnitude and fractal patterns of the Diakonos and Newton methods were evaluated on the Keplerian map, an approximation of the periapsis map, the noisy enclaves observed in the periapsis map disappeared, resulting in a continuous map. This suggests that the convergence characteristics could be further improved if periodic orbits are calculated using the Keplerian map. To achieve this, we aim to refine the approximation of the Keplerian map in future work.

REFERENCES

[1] D. A. Vallado, *Fundamentals of astrodynamics and applications*, Vol. 12. Springer Science & Business Media, 2001.

[2] J. M. James, "Celestial Mechanics Problem Set 2: The State Transition Matrix and Method of Differential Corrections," *rN*, Vol. 1, 2006, p. v2.

[3] Y. Cheung, S. Chen, and S. Lau, "A modified Lindstedt-Poincaré method for certain strongly non-linear oscillators," *International Journal of Non-Linear Mechanics*, Vol. 26, No. 3-4, 1991, pp. 367–378.

[4] M. Lara and J. Peláez, "On the numerical continuation of periodic orbits-an intrinsic, 3-dimensional, differential, predictor-corrector algorithm," *Astronomy & Astrophysics*, Vol. 389, No. 2, 2002, pp. 692–701.

[5] B. I. Epureanu and H. S. Greenside, "Fractal basins of attraction associated with a damped Newton's method," *SIAM review*, 1998, pp. 102–109.

[6] J. Hubbard, D. Schleicher, and S. Sutherland, "How to find all roots of complex polynomials by Newton's method," *Inventiones mathematicae*, Vol. 146, No. 1, 2001, pp. 1–33.

[7] S. D. Ross and D. J. Scheeres, "Multiple gravity assists, capture, and escape in the restricted three-body problem," *SIAM Journal on Applied Dynamical Systems*, Vol. 6, No. 3, 2007, pp. 576–596.

[8] P. Schmelcher and F. Diakonos, "Detecting unstable periodic orbits of chaotic dynamical systems," *Physical Review Letters*, Vol. 78, No. 25, 1997, p. 4733.